3- /\

NRL Report

Detection Strategies for High-Resolution Radar

P. K. HUGHES II

Radar Analysis Branch
Radar Division

March 11, 1982

NAVAL RESEARCH LABORATORY
Washington, D.C.

REPORT DOCUMENTATION PAGE		READ INSTRUCTIONS BEFORE COMPLETING FORM
1. REPORT NUMBER NRL Report 8572	2. GOVT ACCESSION NO.	3. RECIPIENT'S CATALOG NUMBER
4. TITLE (and Subtitle) DETECTION STRATEGIES FOR HIGH-RESOLUTION RADAR		5. TYPE OF REPORT & PERIOD COVERED Interim report on a continuing NRL problem.
		6. PERFORMING ORG. REPORT NUMBER
7. AUTHOR(s) P. K. Hughes II		8. CONTRACT OR GRANT NUMBER(s)
9. PERFORMING ORGANIZATION NAME AND ADDRESS Naval Research Laboratory Washington, DC 20375		10. PROGRAM ELEMENT, PROJECT, TASK AREA & WORK UNIT NUMBERS 62712N; SF12131691; 53-0611-00
11. CONTROLLING OFFICE NAME AND ADDRESS Office of Naval Research Arlington, VA 22217		12. REPORT DATE March 11, 1982
		13. NUMBER OF PAGES 10
14. MONITORING AGENCY NAME & ADDRESS(if different from Controlling Office)		15. SECURITY CLASS. (of this report) UNCLASSIFIED
		15a. DECLASSIFICATION/DOWNGRADING SCHEDULE

16. DISTRIBUTION STATEMENT (of this Report)

Approved for public release; distribution unlimited.

17. DISTRIBUTION STATEMENT (of the abstract entered in Block 20, if different from Report)

18. SUPPLEMENTARY NOTES

19. KEY WORDS (Continue on reverse side if necessary and identify by block number)

Radar
Automatic detection
High-resolution

20. ABSTRACT (Continue on reverse side if necessary and identify by block number)

A comparison of single-range cell detection and integrated contiguous range-cell detection for a high-range resolution radar is presented. A simulation was used to generate probability of detection curves for the two detection strategies using ten target models with different target scattering characteristics. The integrated range-cell detection strategy is superior in all cases except when the target is composed of a single strong flare point.

DD FORM 1473 1 JAN 73   EDITION OF 1 NOV 65 IS OBSOLETE
S/N 0102-014-6601

i

CONTENTS

DETECTION STRATEGIES FOR HIGH-RESOLUTION RADAR

INTRODUCTION

To improve the detection of targets in distributed clutter, one radar technique is to reduce the amount of signal energy backscattered by the clutter. This is accomplished by reducing the range resolution cell of the radar so that fewer scatterers are in the resolution cell of interest. However, when the resolution volume becomes smaller than the target, both the target energy and the clutter energy decrease. Under these circumstances, not only does the detection capability become ambiguous, but how the data should be processed does as well. The reason is that the scattering geometry of the target is unknown and differs significantly from target to target. In this study, detection strategies are investigated for the cases where the resolution cell size of the radar is smaller than the target size, and the target is surrounded by homogeneous distributed clutter.

In most situations, the entire target is covered by the radar beam. Consequently, only the range dimension of the resolution cell can be made smaller than the target size. This is the case to be studied in this report. The range resolution size or *range cell* can be quite small by using modern pulse compression procedures. One other factor of practical importance is that of problems in processing the data rates. Since we are considering range measurements on the order of feet, the samples in time occur a few nanoseconds apart. These short processing times place stiff requirements on the hardware and consequently only simple processors are of practical interest.

We begin by discussing the detection procedures which are evaluated using a Neyman-Pearson criteria.

DETECTION PROCEDURES

In this study we examine two detection strategies for a high-range resolution radar. We select a range bin of 10 ns (about 5 ft in radar range) as the high resolution range cell. The first method involves making a threshold decision every 10 ns and any threshold crossing within a 100-ns window will be declared a detection. In the second method, we will integrate 10 cells and make a threshold decision every 100 ns. As a point of reference, we will also consider the case of a range cell of 100 ns and make threshold decisions every 100 ns. The first method is a special case of the m out of N detector, where $m = 1$. The second method is called the integrated detector.

A block diagram of the radar detection receiver is shown in Fig. 1. In this case, high resolution is obtained by some pulse compression technique. The random variable Z_i represents the ith sample input to the detector. A new Z_i appears at the Constant False Alarm Rate (CFAR) detector every 10 ns. For the reference case, a new sample Z_i is obtained every 100 ns.

An important consideration that cannot be ignored is the target scattering characteristics. Most airborne targets consist of a small number (1 to 6) of distinct scatterers which we shall refer to as flare points. Data [1] exist which indicate that flare points can be resolved within a 5-ft range bin or less. Even large aircraft at most aspect angles contain a small number of these
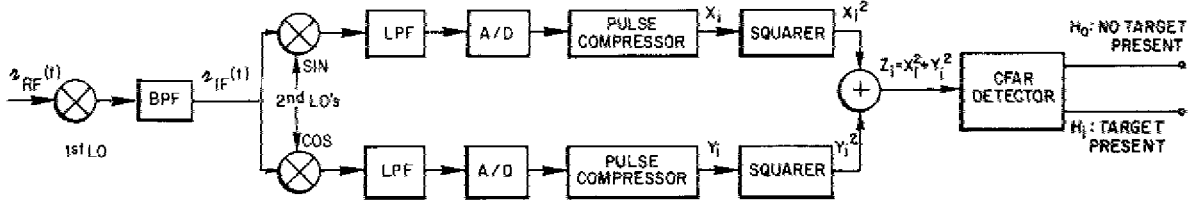

Fig. 1 — Radar receiver

flare points. It is obvious that this target scattering characteristic will affect the detection schemes being considered. The total energy returned from the target can be considered to be the sum of the energy from the target's flare points.

In the next section of this report we consider the statistics of Z_i and determine the detection thresholds for the different detection techniques. Then we discuss the methods used in simulating the problem. Finally, results and conclusions are presented.

THRESHOLD ADJUSTMENT

The clutter is assumed to be much greater than the receiver thermal noise, so thermal noise can be ignored. The clutter will be assumed to be Gaussian distributed with zero-mean, variance σ_c^2, homogeneous, and independent from range cell-to-range cell; therefore, under the *no* signal present hypothesis, X_i and Y_i of Fig. 1 are identically distributed Gaussian random variables with zero-mean, variance σ_c^2, and statistically independent. Then Z_i is a random variable that has an exponential probability distribution function, given by

$$P(Z_i) = \frac{1}{2\sigma_c^2} \exp\left(-Z_i/2\sigma_c^2\right)$$

(1)

$$\text{for } Z_i \geqslant 0 .$$

The probability of a false alarm, P_{fa}, is found by the following equation;

$$P_{fa} = \int_\gamma^\infty P(Z_i)dZ_i ,$$

(2)

where γ is the detection threshold. It follows that γ is the well-known result,

$$\gamma = 2\sigma_c^2 \ln P_{fa} .$$

(3)

The sum of N samples is given by the random variable g, where

$$g = \sum_{j=1}^N Z_j .$$

(4)

Assuming unit variance for X_i and Y_i, the probability distribution function for g is χ^2 with $2N$ degrees of freedom and is given by:

$$P(g) = \frac{1}{2^N \Gamma(N)} g^{N-1} \exp(-g/2)$$

$$\text{for } g \geqslant 0 .$$

(5)

In this case, the probability of a false alarm is given by;

$$P_{fa} = \int_{\gamma}^{\infty} P(g) \, dg ,$$

(6)

where again the γ is the detection threshold. However, in this case γ cannot be found as a simple function of the probability of false alarm. Numerical methods must be used to solve for the detection threshold for a given value of P_{fa}.

Equation (3) provides the threshold for the reference case and the single range cell detection case. Equation (6) provides the threshold for the case where N samples are summed before a threshold decision is made. A plot of probability of false alarm versus the threshold level is shown in Fig. 2 for both the exponential distribution and a χ^2 distribution with 20 degrees of freedom. A more detailed discussion of the above can be found in Ref. 2.
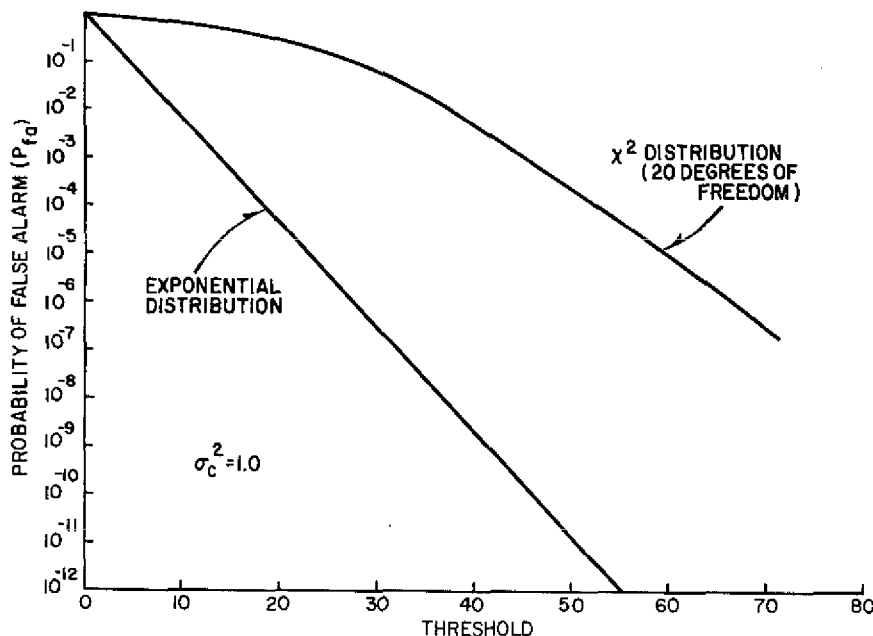

Fig. 2 — Probability of false alarm vs. threshold level

3

PROBABILITY OF DETECTION

The probability of detection for each of the detection procedures was found by simulation. A random number generator was used to obtain clutter samples of X_i and Y_i with a Gaussian distribution. In the simulation the clutter variance for the small range cell was taken as $\sigma_c^2 = 1$; therefore, the 100-ns range cell has a clutter variance of 10. The purpose of the simulation is to determine if there is some *best* detection strategy for high-range resolution waveforms whose range cells are less than the physical extent of typical targets. To accomplish this we generate probability of detection versus signal-to-clutter ratio plots for a given probability of false alarm. The P_{fa} for the 100-ns cell was 10^{-6}. For the 10 ns cell, a P_{fa} of 10^{-7} is used to determine the threshold. Since the m out of N detector will have 10 more opportunities for detecting the target than the integrated detector, its effective P_{fa} is also 10^{-6}.

The target is assumed to lie entirely within the 100-ns range cell. The target flare point locations and the fraction of the total energy returned by each flare point is given in Table 1. The total energy from the target is the sum of the energies from the target's flare points. For the reference case (100-ns range cell) all the flare point echoes are assumed to add in phase.

In the simulation, 1000 signal-plus-clutter samples are generated for each 10-ns range cell for a given total signal level. They are compared to the threshold, and the number of threshold crossings are counted. For the m out of N detector, there are 10 threshold comparisons per target. Multiple detections in the 10 contiguous cells only count as a single detection. This procedure is then repeated for several signal-to-clutter ratios.

RESULTS AND CONCLUSIONS

The results are shown in Figures 3 through 12 for the ten-target models of Table 1. Figure 3 shows for the single flare point target that the m out of N detector is about 10 dB better than the *reference detector*. This was as expected because of the clutter reduction due to improved resolution with no degradation in target energy. It is also about 2 dB better than the integrated detector. The 2 dB can be considered as an integration collapsing loss. Also, the *reference detector* curve which has appeared numerous times in the literature is properly located. However, in Fig. 4, when the target is composed of two equal strength flare points, the m out of N detector becomes 0.2 dB worse than the integrated detector. As seen in Figs. 3 through 12, the integrated detector's performance is independent of the number of target flare points and the amplitude distribution of the flare points. But the m out of N detector is strongly dependent on the target flare points (both their number and amplitude distribution). The more equally dominant flare points there are, the worse the detection performance becomes for the m out of N detector. In Figs. 9 through 11 we note that if there is more than one flare point, but one flare point dominates (i.e., returns more energy to the radar), then the m out of N detector has better detection performance. It appears that if 2/3 or more of the energy returned to the radar from the target comes from a single flare point, then the m out of N detector is better. Otherwise, the integrated cell detector provides better detection performance.

The radar designer can easily decide which strategy to use if he or she is aware of what targets his or her radar will be used to detect. For those without such knowledge, or who must detect a variety of targets, the integration before detection would be the better strategy. The worst case as compared to the single cell detector (with 10 cells integrated for the integration detector) is about a 2 dB collapsing loss.
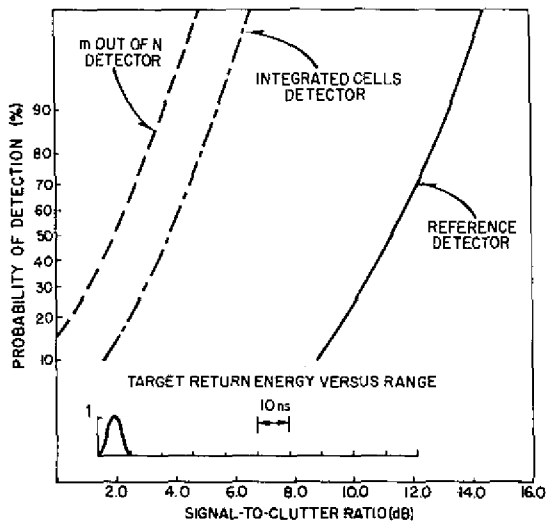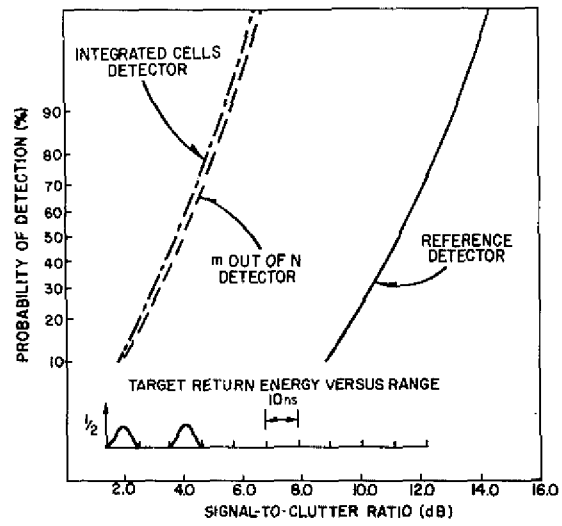
4

Fig. 3 — Target Model No. 1
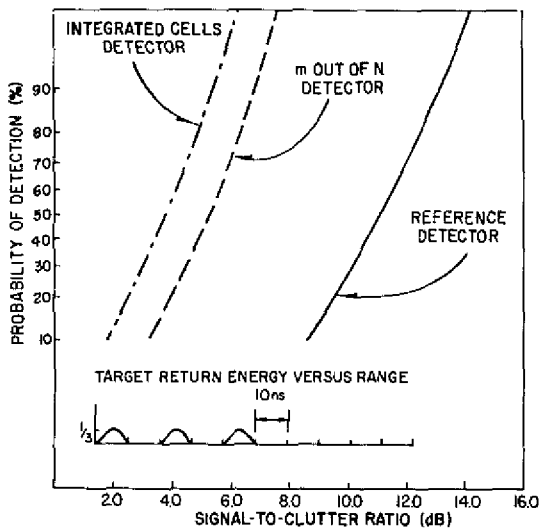

Fig. 4 — Target Model No. 2
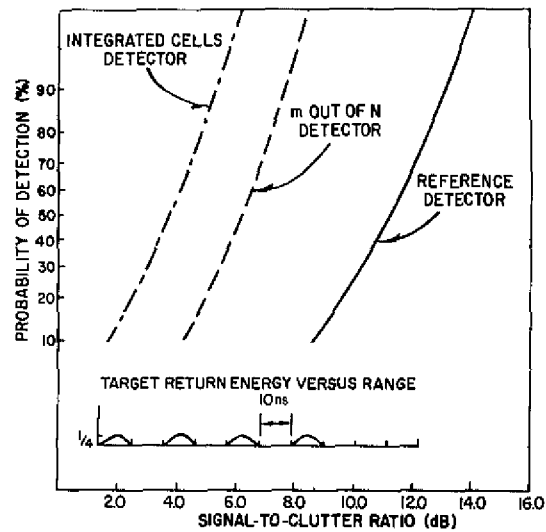

Fig. 5 — Target Model No. 3
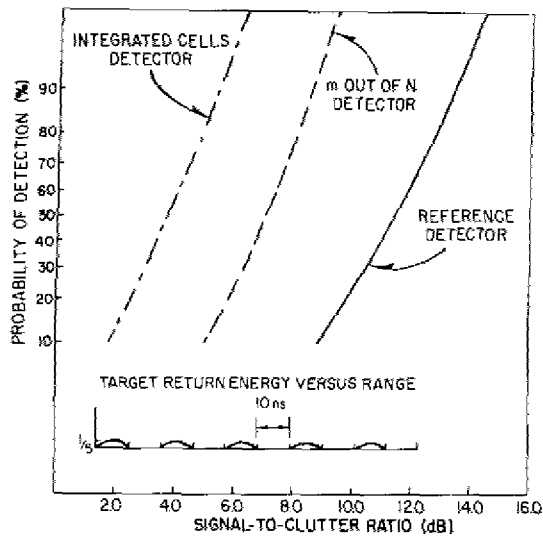

Fig. 6 — Target Model No. 4
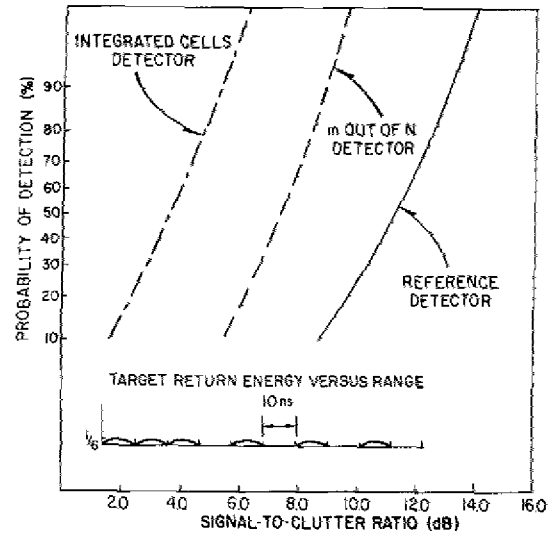
Fig. 7 — Target Model No. 5
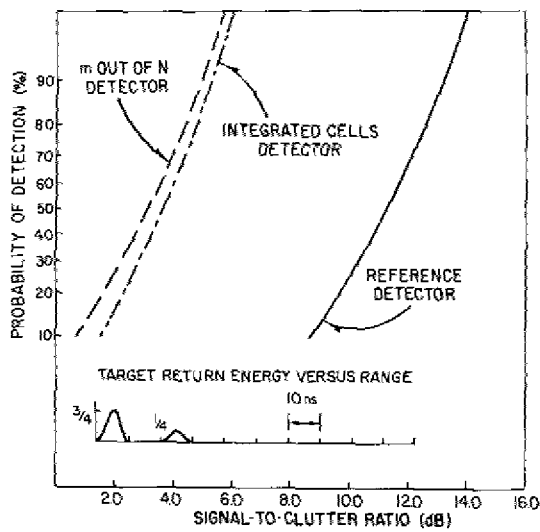

Fig. 8 — Target Model No. 6
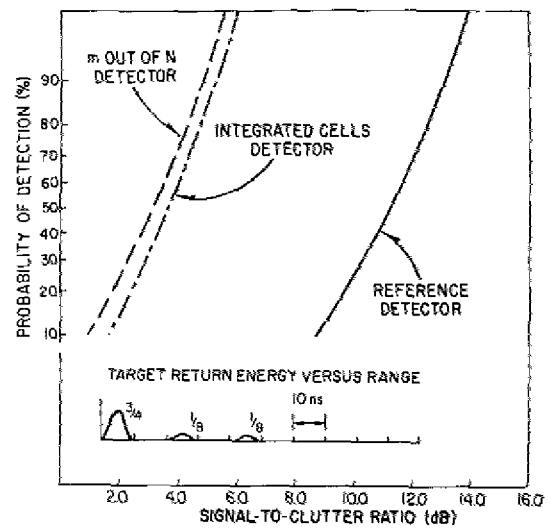

Fig. 9 — Target Model No. 7
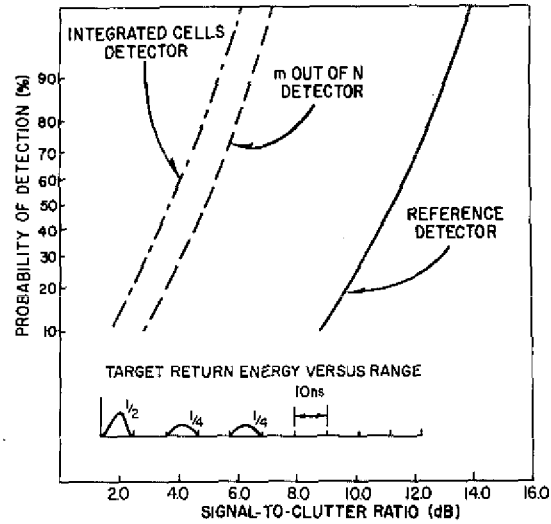

Fig. 10 — Target Model No. 8

Fig. 11 — Target Model No. 9
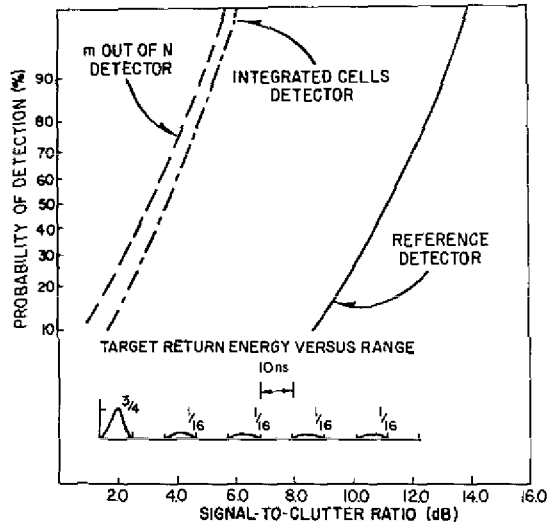

Fig. 12 — Target Model No. 10

Table 1 — Target Models with Flare Point Locations and Percentage of Total Energy
Reflected from Each Flare Point

Model Number	Cell Number									
	1	2	3	4	5	6	7	8	9	10
1	1	0	0	0	0	0	0	0	0	0
2	1/2	0	1/2	0	0	0	0	0	0	0
3	1/3	0	1/3	0	1/3	0	0	0	0	0
4	1/4	0	1/4	0	1/4	0	1/4	0	0	0
5	1/5	0	1/5	0	1/5	0	1/5	0	1/5	0
6	1/6	1/6	1/6	0	1/6	0	1/6	0	1/6	0
7	3/4	0	1/4	0	0	0	0	0	0	0
8	3/4	0	1/8	0	1/8	0	0	0	0	0
9	3/4	0	1/16	0	1/16	0	1/16	0	1/16	0
10	1/2	0	1/4	0	1/4	0	0	0	0	0

SUMMARY

The purpose of this report was to compare a single range cell (m out of N) detector with an integrated range cell detector for high-range resolution radar in the presence of distributed clutter. A simulation was used to generate probability of detection curves of the two detectors for ten target scattering models.

The results indicate that the integrated range-cell detector is superior for all cases except where 2/3 or more of the target's return energy comes from a single highly resolvable flare point. When all the target's return energy comes from a single flare point, the integrated detector is about 2 dB worse than the m out of N detector.

REFERENCES

1. F. D. Queen and J. J. Alter, "Results of a Feasibility Study for Determining the Yaw Angle of a Landing Aircraft," NRL Report 8480, May 27, 1981.

2. A. D. Whalen, *Detection of Signals in Noise*, Academic Press, New York, 1971.